THE EFFECT OF MANUFACTURING TOLERANCES ON THE OPTIMAL DESIGN OF ANISOTROPIC PRESSURE VESSELS

Pavel Y. Tabakov, Mark Walker

Center for Advanced Materials, Design and Manufacturing Research, Durban University of Technology, P.O. Box 953, Durban 4000, South Africa

Abstract

Accurate optimal design solutions for most engineering structures present considerable difficulties due to the complexity and multi-modality of the functional design space. The situation is made even more complex when potential manufacturing tolerances must be accounted for in the optimizing process. The present study provides an original in-depth analysis of the problem and then a new technique for determining the optimal design of engineering structures, with manufacturing tolerances in fiber orientations and layer thicknesses accounted for, is proposed and demonstrated. The numerical examples used to demonstrate the technique involve the design optimization of anisotropic fibre-reinforced laminated pressure vessels. It is assumed that the probability of any tolerance value occurring within the tolerance band, compared with any other, is equal, and thus it is a worst-case scenario approach. A genetic algorithm with fitness sharing, including a micro-genetic algorithm is used and implemented in the technique.

1 Introduction

When engineering structures are manufactured, the design may deviate from their intended design values. These deviations are usually referred to as manufacturing tolerances. Though the deviations can be relatively small, their impact on overall performance of the structure can be significant. It is reasonable that determining the optimal design with manufacturing tolerances accounted for can help to predict accurately such optimal characteristics like maximum applied load or minimum thickness, and by doing so save materials and, perhaps, save the structure from failure.

A few researchers have described methods for dealing with manufacturing tolerances. A pioneering work in this field was published by Chao et al [1] in 1993. This article was the first of its kind to develop a methodology that is focused upon addressing this crucial void in composite materials. Among more recent contributions it is worth mentioning a work of Bauer and Latalski [2] who considered the issue of manufacturing tolerances in dimensions with regard to design optimization, when the objective is minimum weight. A standard solution algorithm with the Kuhn-Tucker theorem is used with a variable method, and the method is illustrated using the standard ten bar benchmark problem; typical for testing algorithms in structural optimization. Liao and Chiou [3] formulated a robust optimum design problem by including the sensitivities and uncertainties in the modified constraints. This method involves both optimization and anti-optimization techniques; however, the anti-optimization sub-problem is solved analytically. In two papers by Walker and Hamilton [4, 5], a technique for optimally designing laminated plates with manufacturing tolerances present in the design variable (which is the fibre orientation) is described. The objective is to maximize the buckling load carrying capacity and in the first, a closed form solution for plates is implemented, whilst in the second, the FEM is used. The techniques are aimed at optimally designing for the worst-case scenario, and the results presented (as a means of illustrating the methodology) demonstrate the importance of accounting for manufacturing uncertainties. A more efficient design optimization algorithm than the one described by Walker and Hamilton is presented in a paper by Tabakov and Walker [6]. The design optimization of anisotropic pressure vessels with manufacturing uncertainties in the fibre orientation (only) accounted for is tackled by way of illustrating the technique. This paper expands on the theme and

focuses on the effect of tolerances in both the fibre orientations and layer thicknesses.

2 Problem description

Consider an arbitrary one-dimensional function $y = f(x)$ of the argument x describing the response of some engineering structure to the change in the argument x (see Fig. 1). The global optimum (maximum in this example) is achieved at $x = x_{opt}^{(nom)}$ on the interval $a \leq x \leq b$ where the solution is feasible. In engineering optimisation a value of x is usually called a design parameter and can be any geometrical or physical property which can be intentionally changed. For example, in a laminated fibre reinforced composite structure it can be a fibre orientation in a layer, the change of which will result in the change of the maximum permissible external load. Evidently in real applications the number of design parameters can be higher than one.
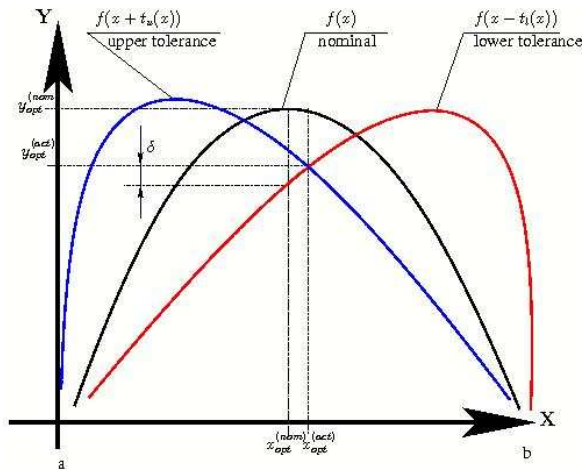
Fig. 1. Effect of manufacturing tolerances on the objective function of an arbitrary 1-D problem.

When engineering structures are manufactured, the design parameters may deviate from their intended design values. These deviations are usually referred to as manufacturing tolerances. Though the deviations can be relatively small, their impact on the overall performance of the structure can be significant. Thus, determining the optimal design with the manufacturing tolerances accounted for can help to predict accurately such optimal characteristics like maximum applied load or minimum thickness, and by doing so save materials and, perhaps, save the structure from failure.

Fig. 1 demonstrates how the actual value of a design parameter can be determined. The solid line shows the nominal function, which is the intended design; the two other trendlines represent the cases of possible deviations, namely upper and lower tolerance. The actual value of the design parameter will correspond to the coordinate of the point where these two graphs intersect. In such a case $x_{opt}^{(act)}$ can be either greater or less than $x_{opt}^{(nom)}$ whereas the function value is always $y_{opt}^{(act)} \leq y_{opt}^{(nom)}$ in the maximization problem or $y_{opt}^{(act)} \geq y_{opt}^{(nom)}$ in the case of finding the global minimum. It can be seen from the figure that the actual parameter $x_{opt}^{(act)}$ must be used for design purposes. In this case the value of the function will not drop below $y_{opt}^{(act)}$, which corresponds to the worst-case scenario. However, if the value $x_{opt}^{(nom)}$ of the design parameter is used, then in the worst case scenario the magnitude of the function will drop even more, namely by the value of δ (see Fig. 1). Understanding this presents a fundamental issue in analysis of structures that may have manufacturing tolerances when constructed.

As Fig. 1 suggests, the evaluation of the intersection point in a one-dimensional optimisation problem presents no special difficulties. However, this problem becomes rather complicated with an increase in the dimensionality of the objective function. Geometrically, the domain of points representing the intersection of two sister functions is a hyper-surface of the dimension $N - 1$, where N is the dimension of the objective function. For example, in the case of a two-dimensional problem it will be a line, three-dimensional is a surface, four and more dimensions is a hyper-surface. The optimal solution is found on this line, surface or hyper-surface provided it is a common domain for all the functional (hyper-) surfaces. We would call such a domain the solution line or solution (hyper-) surface, depending on the considered problem. It is reasonable to assume that multimodal estimation of the actual global optimum of such problems is difficult to accomplish, especially for higher-dimensional problems, due to the curse of dimensionality. Moreover, the number of intersecting functional surfaces increases exponentially as the dimensionality of the problem increases. Generally, if there is a probability that every design parameter can experience deviation

from its intended value in either direction, the number of such surfaces will be 2N. While in the simplest case of a one-dimensional problem only two lines intersect (the nominal case is not taken into account), in the case of two dimensions we have already four surfaces, which are

$$f_{uu} = f(x + t_u(x), y + t_u(y))$$
$$f_{ll} = f(x - t_l(x), y - t_l(y))$$
$$f_{ul} = f(x + t_u(x), y - t_l(y))$$
$$f_{lu} = f(x - t_l(x), y + t_u(y))$$

(1)

Where t_u and t_l are upper and lower tolerances respectively. To gain a better understanding of how the solution line is formed in the previous example we shall use ellipses to illustrate schematically, as shown in Fig. 2. The thick bold line (view from the top) here is the common intersection line for all the four surfaces considered. The solution will be the maximum (or minimum) point on this line. Obviously, in a real problem this looks different but the geometrical principle is the same.
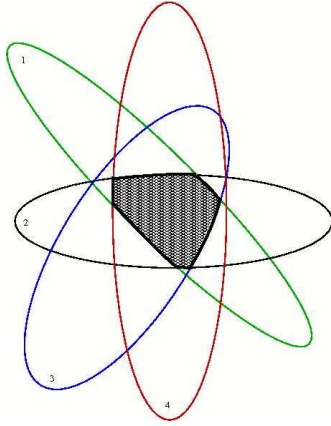
Fig. 2.Schematic demonstrating the solution line in a 2-D design problem.

3 Laminated Pressure Vessels

Fibre-reinforced laminated structures are probably the most tolerance-prone of engineering structures because of the fabrication technologies used. These structures are manufactured as the material is fabricated from constituents, viz. reinforcing fibres and a plastic matrix, which must be cured as part of the processing. This can often lead to deviations from the intended design, particularly with regard the fibre orientations. In order to illustrate the methodology described above

we consider a rather complex engineering problem: finding the burst pressure in a laminated anisotropic cylindrical pressure vessel of finite length using an exact elasticity solution (see Fig. 3). The cylinder is constructed of filament-wound layers with a fibre orientation of $\pm\theta°$. The axis of anisotropy coincides with the axis of symmetry Oz of the cylinder and the stresses act on the planes normal to the generator. Unfortunately, the mathematical foundations of the analysis are quite cumbersome and thus only are basic equations are given next in order to help the reader better understand the theory used. The interested reader can find the detailed solution in [7] or should contact the authors.
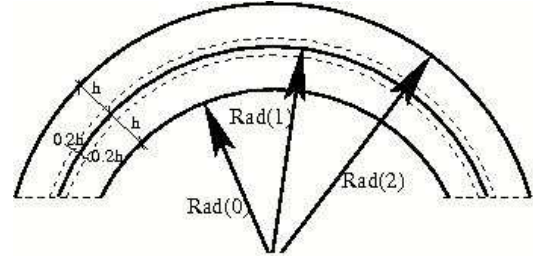
Fig. 3. Geometry of an anisotropic cylindrical pressure vessel.

3.1 Computation of stresses

The distribution of the stresses will be identical in all cross sections and will depend only on the distance r from the axis. Therefore, for every layer k the stresses are expressed in terms of stress functions proposed by Lekhnitskii [8] $\Phi_k = \Phi_k(r), \Psi_k = \Psi_k(r)$ as

$$\sigma_r^{(k)} = \frac{1}{r}\frac{d\Phi_k}{dr}; \sigma_\phi^{(k)} \frac{d^2\Phi_k}{dr^2}; \tau_{\phi z}^{(k)} = -\frac{d\Psi_k}{dr} \quad (2)$$

and longitudinal stresses

$$\sigma_z^{(k)} = C - \frac{1}{\alpha_{33}^{(k)}}\left(\alpha_{13}^{(k)}\sigma_r^{(k)} + \alpha_{23}^{(k)}\sigma_\phi^{(k)} + \alpha_{34}^{(k)}\tau_{\phi z}^{(k)}\right) \quad (3)$$

Moreover, due to symmetry

$$\tau_{rz}^{(k)} = \tau_{r\phi}^{(k)} = 0 \quad (4)$$

The boundary conditions on the internal ($r = a_0$) and external ($r = a_{nl}$) surfaces are specified as

$$\sigma_r^{(1)}(a_0) = -p_0; \sigma_r^{(nl)}(a_{nl}) = -p_{nl} \quad (5)$$

At the contact surfaces of adjacent layers we have the following conditions

$$\sigma_r^{(k)} = \sigma_r^{(k+1)}; u_r^{(k)} = u_r^{(k+1)}; u_\phi^{(k)} = u_\phi^{(k+1)} \quad (6)$$

The equilibrium of forces on the end surfaces gives

$$2\pi\sum_{k=1}^{nl}\int_{a_{k-1}}^{a_k}\sigma_z^{(k)}rdr = \pi(p_0 - p_{nl})a_0^2 + F \qquad (7)$$

where F is the applied axial force.

With the regards to the conditions (6) and taking into account the assumptions on physical and geometrical properties given above, the general solution has the following form [8]:

$$\Phi_k = C\varsigma_1^{(k)}\frac{r^2}{2} + \frac{C_1}{1+\kappa_k}r^{1+\kappa_k} + \frac{C_2}{1-\kappa_k}r^{1-\kappa_k}$$

$$\Psi_k = Cr\left(\frac{\alpha_{34}^{(k)}}{\beta_{44}^{(k)}} + \varsigma_1^{(k)}g_1^{(k)}\right) + \frac{C_1}{1+\kappa_k}g_\kappa^{(k)}r^{1+\kappa_k} \qquad (8)$$

$$- C_2\frac{1}{\kappa_k}g_{-\kappa}^{(k)}r^{-\kappa_k}$$

where $\varsigma_1^{(k)}$, κ_k, $g_1^{(k)}$, $g_\kappa^{(k)}$ and $g_{-\kappa}^{(k)}$ are β-dependent coefficients, and $\beta_{ij}^{(k)}$ are elastic constants given by

$$\beta_{ij}^{(k)} = \alpha_{ij}^{(k)} - \frac{\alpha_{i3}^{(k)}\alpha_{j3}^{(k)}}{\alpha_{33}^{(k)}}, \quad i,j = 1,2,4 \qquad (9)$$

$$\varsigma_1^{(k)} = \frac{(\alpha_{13}^{(k)} - \alpha_{23}^{(k)})\beta_{44}^{(k)} - \alpha_{34}^{(k)}(\beta_{14}^{(k)} - \beta_{24}^{(k)})}{\beta_{22}^{(k)}\beta_{44}^{(k)} - \beta_{24}^{(k)2} - (\beta_{11}^{(k)}\beta_{44}^{(k)} - \beta_{14}^{(k)2})}$$

$$\kappa_k = \sqrt{\frac{\beta_{11}^{(k)}\beta_{44}^{(k)} - \beta_{14}^{(k)2}}{\beta_{22}^{(k)}\beta_{44}^{(k)} - \beta_{24}^{(k)2}}}; \quad g_1^{(k)} = \frac{\beta_{14}^{(k)} + \beta_{24}^{(k)}}{\beta_{44}^{(k)}} \qquad (10)$$

$$g_k^{(k)} = \frac{\beta_{14}^{(k)} + \kappa_k\beta_{24}^{(k)}}{\beta_{44}^{(k)}}; \quad g_{-k}^{(k)} = \frac{\beta_{14}^{(k)} - \kappa_k\beta_{24}^{(k)}}{\beta_{44}^{(k)}}$$

The stresses can be calculated from Eq. 2 as

$$\sigma_r^{(k)}C\varsigma_1^{(k)} + C_1r^{\kappa_k-1} + C_2r^{-\kappa_k-1}$$

$$\sigma_\phi^{(k)}C\varsigma_1^{(k)} + C_1\kappa_k r^{\kappa_k-1} - C_2\kappa_k r^{-\kappa_k-1} \qquad (11)$$

$$\tau_{\phi z}^{(k)} = -C\left(\frac{\alpha_{34}^{(k)}}{\beta_{44}^{(k)}} - \varsigma_1^{(k)}g_1^{(k)}\right) - C_1g_k^{(k)}r^{\kappa_k-1}$$

$$- C_2g_{-k}^{(k)}r^{-\kappa_k-1}$$

By satisfying the boundary conditions (5) and (6) the constants C_1 and C_2 can be expressed in terms of the constant C. By introducing the notations

$$c_k = \frac{a_{k-1}}{a_k}; \quad \rho_k = \frac{r}{a_k} \quad (c_k < 1, c_k \le \rho_k \le 1) \qquad (12)$$

the final expressions for the stresses can be written as

$$\sigma_r^{(k)} = \frac{p_{k-1}c_k^{\kappa_k+1} - p_k}{1-c_k^{2\kappa_k}}\rho_k^{\kappa_k-1}$$

$$+ \frac{p_k c_k^{\kappa_k-1} - p_{k-1}}{1-c_k^{2\kappa_k}}c_k^{\kappa_k+1}\rho_k^{-\kappa_k-1} + C\varsigma_1^{(k)}W_1^{(k)}$$

$$\sigma_\phi^{(k)} = \frac{p_{k-1}c_k^{\kappa_k+1} - p_k}{1-c_k^{2\kappa_k}}\kappa_k\rho_k^{\kappa_k-1} \qquad (13)$$

$$- \frac{p_k c_k^{\kappa_k-1} - p_{k-1}}{1-c_k^{2\kappa_k}}\kappa_k c_k^{\kappa_k+1}\rho_k^{-\kappa_k-1} + C\varsigma_1^{(k)}W_2^{(k)}$$

$$\tau_{\phi z}^{(k)} = -\frac{p_{k-1}c_k^{\kappa_k+1} - p_k}{1-c_k^{2\kappa_k}}g_k^{(k)}\rho_k^{\kappa_k-1}$$

$$- \frac{p_k c_k^{\kappa_k-1} - p_{k-1}}{1-c_k^{2\kappa_k}}g_{-k}^{(k)}c_k^{\kappa_k+1}\rho_k^{-\kappa_k-1} + CW_3^{(k)}$$

where

$$W_1^{(k)} = 1 - \frac{1-c_k^{\kappa_k+1}}{1-c_k^{2\kappa_k}}\rho_k^{\kappa_k-1} - \frac{1-c_k^{\kappa_k-1}}{1-c_k^{2\kappa_k}}c_k^{\kappa_k+1}\rho_k^{-\kappa_k-1}$$

$$W_2^{(k)} = 1 - \frac{1-c_k^{\kappa_k+1}}{1-c_k^{2\kappa_k}}\kappa_k\rho_k^{\kappa_k-1} + \frac{1-c_k^{\kappa_k-1}}{1-c_k^{2\kappa_k}}\kappa_k c_k^{\kappa_k+1}\rho_k^{-\kappa_k-1}$$

$$W_3^{(k)} = \zeta_2^{(k)} + \zeta_1^{(k)}\left(\frac{1-c_k^{\kappa_k+1}}{1-c_k^{2\kappa_k}}g_k^{(k)}\rho_k^{\kappa_k-1}\right.$$

$$\left. + \frac{1-c_k^{\kappa_k-1}}{1-c_k^{2\kappa_k}}g_{-k}^{(k)}c_k^{\kappa_k+1}\rho_k^{-\kappa_k-1}\right)$$

$$\zeta_2^{(k)} = \frac{(\alpha_{13}^{(k)} - \alpha_{23}^{(k)})(\beta_{14}^{(k)} + \beta_{24}^{(k)}) - \alpha_{34}^{(k)}(\beta_{11}^{(k)} - \beta_{22}^{(k)})}{\beta_{22}^{(k)}\beta_{44}^{(k)} - \beta_{24}^{(k)2} - (\beta_{11}^{(k)}\beta_{44}^{(k)} - \beta_{14}^{(k)2})}$$

In Eq. 13 p_{k-1} and p_k denote the normal forces acting on internal and external surfaces of the k-th layer. The remaining unknown forces and constant C are determined from the boundary conditions (6) and (7). Next, the system of equations for the calculation of the unknown interface forces $p_1, p_2,..., p_{nl-1}$ and the constant of integration C are derived. The first nl - 1 equations of the system of equations are derived by satisfying the displacement continuity conditions at the interfaces, i.e.

$$\varepsilon_\phi^{(k)} = \varepsilon_\phi^{(k+1)} \quad \text{at } r = a_k \qquad (14)$$

which gives us the following system of nl-1 equations

4

$$\varepsilon_\phi^{(k)} - \varepsilon_\phi^{(k+1)} = 0, \quad k = 1,2,\ldots,nl-1 \qquad (15)$$

for p_k, where

$$\varepsilon_\phi^{(k)} = \alpha_{12}^{(k)}\sigma_r^{(k)} + \alpha_{22}^{(k)}\sigma_\phi^{(k)} + \alpha_{23}^{(k)}\sigma_z^{(k)} + \alpha_{24}^{(k)}\tau_{\phi z}^{(k)} \ (16)$$

By substituting the above expressions into the equations for the boundary conditions (15), and after rearranging terms and simplification, we arrive at the set of equations for unknown forces and the constant of integration C in the following form:

$$p_{k-1}\Delta_2^{(k)} + p_k(\Delta_3^{(k)} - \Delta_2^{(k+1)}) + p_{k+1}\Delta_3^{(k+1)}$$
$$= -C(\Delta_1^{(k)} - \Delta_1^{(k+1)}) \qquad (17)$$

The unknown coefficients Δ's are computed with the help of the equations for the stresses (13) and are not listed here.

The total number of unknown terms in the system of equations (17) is equal to the number of the layers nl, whereas the number of equations is nl-1. Therefore, in order to solve this system we need one more equation, namely Eq. 7 which contains the piecewise integral. After the integration the additional equation can be written in the following form

$$\sum_{k=1}^{nl}\left(p_{k-1}\lambda_1^{(k)} + p_k\lambda_2^{(k)} + C\lambda_3^{(k)}\right) = \pi(p_0 - p_{nl})a_0^2 + F \ (18)$$

Unlike the system (17), the expression (18) represents only a single equation calculated as a sum through the thickness, with k varying from 1 to nl. The derivation and the representation of the coefficients λ's is rather complicated and is not presented in this paper.

In order to get better understanding of the system of governing equations, we express it in matrix form:

$$\{B\}\{P\} = \{R\}$$

where the coefficients b_{ij}, r_i $(i, j = 1,2,\ldots,nl)$ are computed from Eq. 17 and 18. It should be noted that in general $b_{ij} \neq b_{ji}$. All the terms Δ's and λ's (which include coefficients ρ's) depend on the point where they are calculated within the thickness of the layer, namely at the bottom or at the top of the layer. Therefore, to distinguish them we shall use indices b for bottom and t for top. Then the coefficients b_{ij} can be defined as:

- The first row

$$b_{11} = \Delta_{3,t}^{(1)} + \Delta_{2,b}^{(2)}; \quad b_{21} = \Delta_{3,b}; \quad b_{1,nl} = \Delta_{1,t}^{(1)} - \Delta_{1,b}^{(2)}$$

- The rows from $i = 2$ to $i = nl - 2$

$$b_{i,i-1} = \Delta_{2,t}^{(i)}; \quad b_{i,i} = \Delta_{3,t}^{(i)} + \Delta_{2,b}^{(i+1)}$$

$$b_{i,i+1} = \Delta_{3,b}^{(i+1)}; \quad b_{i,nl} = \Delta_{1,t}^{(i)} - \Delta_{1,b}^{(i+1)}$$

- The penultimate row

$$b_{nl-1,\ nl-2} = \Delta_{2,t}^{(nl-1)}; \quad b_{nl-1,\ nl-1} = \Delta_{3,t}^{(nl-1)} + \Delta_{2b}^{(nl)}$$

$$b_{nl-1,\ nl} = \Delta_{1,t}^{(nl-1)} - \Delta_{1b}^{(nl)}$$

- The last row

$$b_{nl,i} = \lambda_1^{(i)} + \lambda_2^{(i+1)} \quad (i = 1,2,\ldots,nl-1)$$

$$b_{nl,nl} = \sum_{i=1}^{nl}\lambda_3^{(i)}$$

The right-hand side vector usually contains only three nonzero components if there are both the internal and external pressures applied, which are

$$r_1 = -p_0\Delta_{2,t}^{(1)}; \quad r_{nl-1} = -p_{nl}\Delta_{3,b}^{nl}$$

$$r_{nl} = -p_0\lambda_1^{(1)} - p_{nl}\lambda_2^{(nl)} + \pi(p_0 - p_{nl})a_0^2 + F$$

Finally, it should be noted that when the winding angle $\theta_k = 0°$ or $90°$ we are dealing with an orthotropic layer with cylindrical anisotropy, which means that there are two planes of elastic symmetry, radial and tangential. Then $\alpha_{34}^{(k)} = \beta_{14}^{(k)} = \beta_{24}^{(k)} = g_k^{(k)} = g_{-k}^{(k)} = 0$ and tangential stresses $\tau_{\phi z}^{(k)}$ vanish. In the case when $\theta_k = 0°$

$$\kappa_k = \sqrt{\frac{\beta_{11}^{(k)}}{\beta_{22}^{(k)}}} = 1 \qquad (19)$$

and some denominators containing κ_k become equal to zero that leads to singularity. In actual computation, this difficulty can be overcome by assigning a very small number for θ_k (e.g. 0.001°) when $\theta_k = 0°$.

3.2 Failure criterion

The strength of filamentary composites is determined by the tensile and comprehensive strengths in the fibre directions and by the shear strength of the composite material. Failure in tension usually occurs when the fibers break, whereas failure in compression involves debonding of the fibres and the matrix material as a result of micro-buckling. Failure in shear is usually characterized by crack propagation through the composite material. In composite structures, tensile,

comprehensive and shear stresses may result even from simple loading conditions, and therefore the failure mode of composite structures is rather complicated.

Using the Tsai-Wu failure criterion [9] we attempt to calculate the maximum burst pressure with respect to the fibre orientations in the layers and taking into account the manufacturing tolerances. The assumption of the Tsai-Wu three-dimensional failure criterion is that there exists a failure surface in the stress space expressed in the following scalar form

$$f(\sigma_k) = F_i\sigma_i + F_{ij}\sigma_i\sigma_j = 1 \qquad (20)$$

where $k, i, j = 1, 2, \ldots, 6$; F_i and F_{ij} are strength tensors of the second and forth rank, respectively. It is noted that this equation is applied to each layer to check for failure or otherwise. In case of laminated pressure vessels possessing cylindrical anisotropy, Eq. 20 for the k-th layer can be written in the following expanded form:

$$F_{11}^{(k)}\sigma_1^{(k)2} + F_{33}^{(k)}(\sigma_3^{(k)2} + \sigma_2^{(k)2}) + F_{44}^{(k)}\tau_{12}^{(k)2}$$
$$+ 2F_{31}^{(k)}(\sigma_3^{(k)} + \sigma_2^{(k)})\sigma_1^{(k)} + 2F_{32}^{(k)}\sigma_3^{(k)}\sigma_2^{(k)} \qquad (21)$$
$$+ F_3^{(k)}(\sigma_3^{(k)} + \sigma_2^{(k)}) + F_1^{(k)}\sigma_1^{(k)} - 1 = 0$$

where

$$F_{11}^{(k)} = \frac{1}{X_t^{(k)}X_c^{(k)}}; F_{33}^{(k)} = \frac{1}{Y_t^{(k)}Y_c^{(k)}}; F_{44}^{(k)} = \frac{1}{S^{(k)2}}$$

$$F_3^{(k)} = \frac{1}{Y_t^{(k)}} - \frac{1}{Y_c^{(k)}}; F_1^{(k)} = \frac{1}{X_t^{(k)}} - \frac{1}{X_c^{(k)}}$$

$$F_{31}^{(k)} = -\frac{1}{2}\sqrt{F_{33}^{(k)}F_{11}^{(k)}}; F_{32}^{(k)} = -\frac{1}{2}F_{33}^{(k)}$$

and X_t, X_c are, respectively, longitudinal tensile and compressive strengths, Y_t, Y_c are those for the transverse direction and S is the shear strength. It should be noted that the normal stresses $\sigma_i^{(k)}$, $i = 1,2,3$ and shear stress $\tau_{12}^{(k)}$ are stresses in the material coordinates and can be computed as

$$\sigma_1^{(k)} = \sigma_z^{(k)}\cos^2\theta_k + \sigma_\phi^{(k)}\sin^2\theta_k - \tau_{\phi z}^{(k)}\sin 2\theta_k$$
$$\sigma_2^{(k)} = \sigma_z^{(k)}\sin^2\theta_k + \sigma_\phi^{(k)}\cos^2\theta_k + \tau_{\phi z}^{(k)}\sin 2\theta_k$$
$$\sigma_3^{(k)} = \sigma_r^{(k)} \qquad (22)$$
$$\tau_{12}^{(k)} = (\sigma_\phi^{(k)} - \sigma_z^{(k)})\sin\theta_k\cos\theta_k - \tau_{\phi z}^{(k)}\cos 2\theta_k$$

The design objective is the maximization of the burst pressure P_{cr} subject to the failure criterion Eq. 20. The design problem for a multilayered pressure vessel of a given thickness ratio b/a and number of layers nl can be stated as

$$P_{max} \propto \max_\Theta P_{cr}(\Theta, r) = \max_\Theta \min_r P_{cr} \qquad (23)$$

where $\Theta = \{\theta_1, \theta_2, \theta_3, \ldots, \theta_{nl}\}^T$ and $P_{cr}(\Theta, r)$ can be easily calculated from the quadratic equation

$$(F_{ij}\sigma_i^{(k)}\sigma_j^{(k)})P_{cr}^{(k)2} + (F_i\sigma_i^{(k)})P_{cr}^{(k)} - 1 = 0 \qquad (24)$$

where the stresses are calculated for an applied unit pressure $P_{cr}(\Theta, r) = \min_k P_{cr}^{(k)}$. Solution of Eq. 24 gives

$$P_{cr}^{(k)} = -\left(\frac{\zeta^{(k)}}{2\delta^{(k)}}\right) + \sqrt{\left(\frac{\zeta^{(k)}}{2\delta^{(k)}}\right)^2 + \frac{1}{\delta^{(k)}}} \qquad (25)$$

where

$$\delta^{(k)} = F_{33}^{(k)}(\sigma_3^{(k)2} + \sigma_2^{(k)2}) + 2F_{32}^{(k)}\sigma_3^{(k)}\sigma_2^{(k)}$$
$$+ 2F_{31}^{(k)}(\sigma_3^{(k)} + \sigma_2^{(k)})\sigma_1^{(k)} + F_{11}^{(k)}\sigma_1^{(k)2} + F_{44}^{(k)}\tau_{12}^{(k)2}$$
$$\zeta^{(k)} = F_3^{(k)}(\sigma_3^{(k)} + \sigma_2^{(k)}) + F_1^{(k)}\sigma_1^{(k)}$$

The negative root for $P_{cr}^{(k)}$ does not have any physical meaning and the positive value only must be taken into consideration.

The optimization procedure involves the stages of iteratively improving $\theta_{opt}^{(k)}, k = 1,2,\ldots,nl$ in order to maximize P_{cr} for a given radius and thickness ratio.

4 Optimization

For the purpose of visual illustration we use one and two layers, but the approach used is the same for any number of design parameters (layers) except that the nesting algorithm should be used for higher dimensions. The ratio of the external radius to internal in the cylinder used in the example is $b/a = 1.1$ while the length is arbitrary. The material properties are those for a typical T300/5208 graphite/epoxy material: $E_1 = 1.811 \times 10^5$MPa, $E_2 = 1.03 \times 10^4$MPa, $G_{12} = 7.17 \times 10^3$MPa, $\nu_{12} = 0.2897$.

4.1 Uncertainties in fiber orientations

Furthermore, we assume that on the interval [$0° \leq \theta \leq 90°$] the desired fibre orientation in the layer may deviate from its intended design value by $t_u = 13°$ and $t_l = 7°$, which are upper and lower tolerances, respectively.
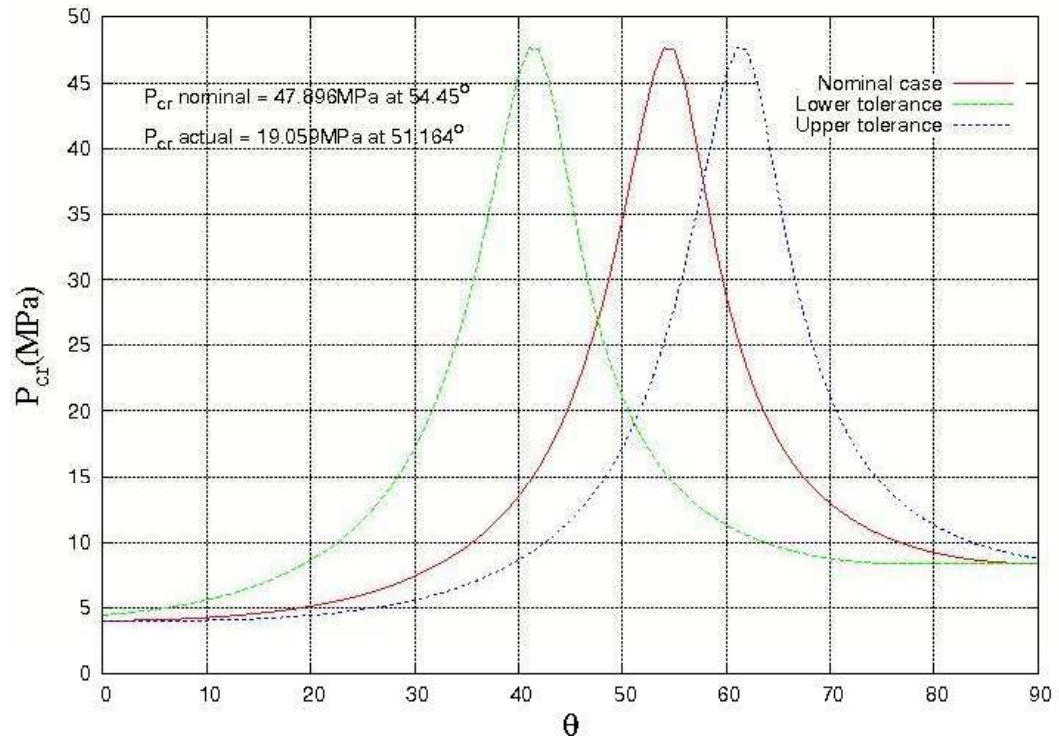
Fig.4. Effect of manufacturing tolerances on the burst pressure of pressure vessel with one ply.
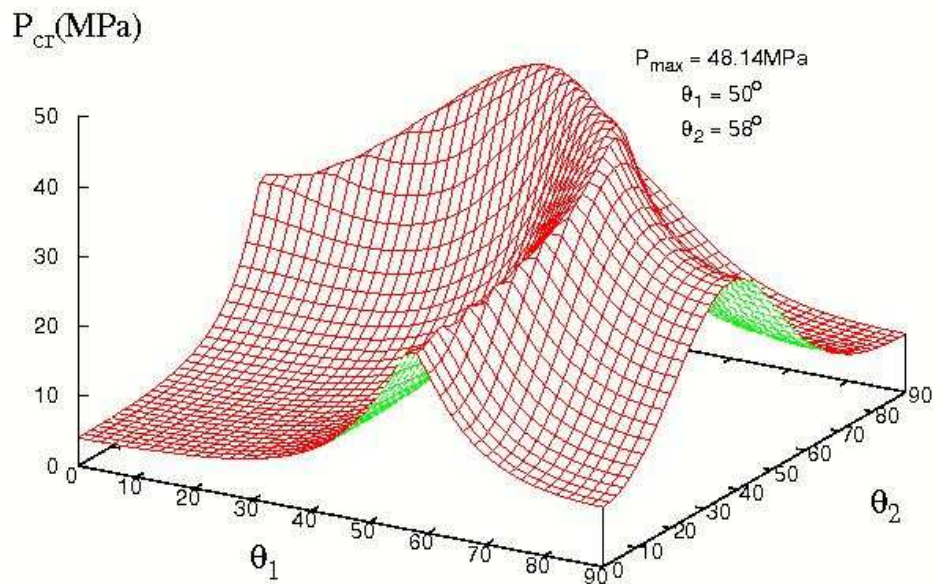
Fig.5. Distribution of the nominal burst pressure of pressure vessel with two plies.
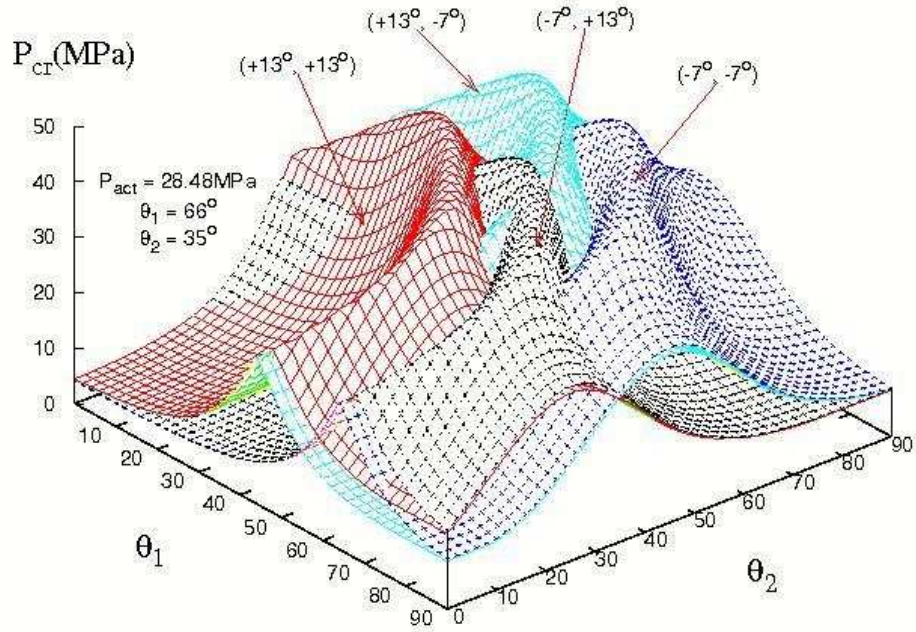
Fig.6. Effect of manufacturing tolerances in fibre orientations on the burst pressure with two plies.
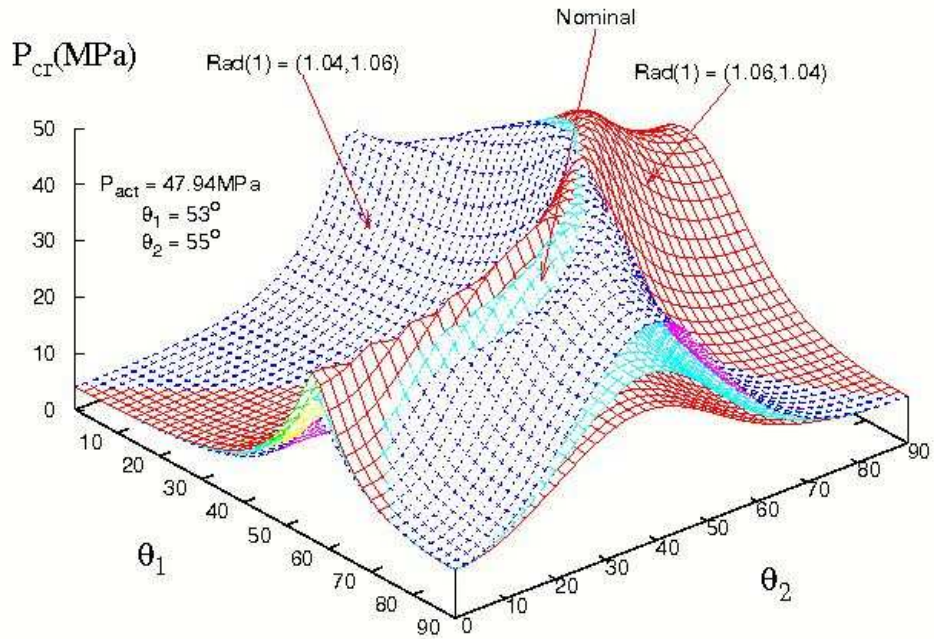
Fig.7. Effect of manufacturing tolerances in layer thicknesses on the burst pressure with two plies.

In reality, the probability of any tolerance value within the tolerance band is variable, usually higher when closer to 0° or 90° and smaller in between. For simplicity, we ignore this fact, as it is irrelevant for the demonstration of the technique.

Fig. 4 shows three trendlines which represent the nominal case (*viz.* critical pressure P_{cr} = 47.90 MPa at the angle θ = 54.45° along with the upper and lower bounds (*viz* the values at $\theta + t_u$ and $\theta - t_l$) and clearly demonstrates how dangerous the manufacturing tolerances can be should they occur during the manufacture of the pressure vessel. It can be also seen from the figure how sensitive the burst pressure is to the change in the fibre orientation. The intersection point of the upper and lower tolerance trendlines clearly indicates the new value of the angle θ =51.16° which must be chosen instead of the nominal value when the cylinder is manufactured. We discover that the actual value of the burst pressure drops from the nominal one by 60.21% to 19.06MPa. Furthermore, if we were to specify the nominal value of the orientation and yet during fabrication tolerances were incurred, the burst pressure could be as low as 14.99MPa (at 54.45+13°), which is 69% lower than the expected (nominal) value. Although fractions of degrees usually are not taken into account by the manufacture, for academic purposes we calculated the exact value of the maximum critical pressure and the relevant angles.

Fig. 5 shows the dependence of the burst pressure in the two-layered cylinder in the case when no manufacturing tolerances occur (nominal case). The exact critical pressure in this case is P_{cr} = 48.14MPa found at θ_1 = 50.06° and θ_2 = 57.88°. Applying the manufacturing tolerances t_u = 13° and t_l = 7° we obtain the four surfaces shown in Fig. 6 and after optimisation the actual value of the burst pressure is determined as 28.48MPa at θ_1 = 66.11° and θ_2 =34.70°. This burst pressure has dropped by 40.84%. Again, to show the significance, if we were to specify the nominal fibre orientations and if tolerances were incurred during manufacture, the burst pressure could be as low as 15.32MPa, which is 68% less than the expected (nominal) value.

For a final comparison, in the case of five-layered cylinder the nominal value of the maximum burst pressure is 51.45MPa found at 46.41/45.79/45.72/49.77/75.37 degrees. After applying the tolerances we arrive at the actual value of the critical pressure of 32.85MPa found at 90.00/32.71/65.38/35.14/37.26 degrees. Here the difference is 36.16%. This example clearly demonstrates how important it is to take the manufacturing tolerances into account in the design optimisation stage. It also illustrates that it is much safer to use a few layers instead of one. However, calculations show that after about 10 layers there is not much improvement in the performance of the pressure vessel. Finally, to again emphasize the importance of including the manufacturing uncertainty, if we specify the nominal and during fabrication tolerances are incurred, the worst case scenario would result in a burst pressure of 18.31 MPa, which is 64% less than the actual.

4.2 Uncertainties in Layer Thicknesses

It is apparent that if the thickness gets smaller the strength of the pressure vessel will decrease and this scenario must be taken into account at a design stage. The deviation in the bigger direction should not worry us much from a structural point of view; however, there is a concern about the total weight and the amount of the material used.

As an example we consider only a two-layered special case where the total thickness of the layer package is constant, but the thicknesses of individual layers can deviate from their original design up to 20%. Again, we consider only the worst case scenario, where only the most extreme parameters are taken into account. Fig. 7 demonstrates the case when there are manufacturing uncertainties in the layer thicknesses and no uncertainties in the fibre orientations. Contrary to the previous example the calculations show that there is no sharp drop in the critical pressure when comparing with the nominal case: P_{cr}.= 47.94MPa at 53.29°/55.23°. However, if all the uncertainties, in fibre orientations and layer thicknesses, occur simultaneously, the impact of the uncertainties in layer thicknesses becomes more pronounced: P_{cr} = 23.26MPa at 66.82°/33.28°, which is 18% less than the case with the uncertainties occurring only in the fibre orientation. Unfortunately, due to complexity, this example cannot be graphically presented.

The computational time for the analysis in this example is of no concern because a closed-form solution used, but this is not the case when the solution is based on a complex finite element analysis. In such cases, a high number of function evaluations might become a critical factor. Therefore, the optimising algorithm should be as

efficient as possible. In our case we used a high number of iterations to obtain the optimum solution, or very close to it. With a population of 50 the maximum number of iteration was 10,000, which amounts to 500,000 function evaluations. In reality there is no need for such a high number of function evaluations; about 95-98% of the accuracy is already achieved after 1,000 iterations. It also should be noted that the optimising procedure is used only once for each structure under consideration, before manufacturing takes place, and the time invested in the analysis is paid off later.

5 Conclusions

In this paper, a new generalized technique for optimally designing engineering structures with manufacturing tolerances in the design variables is presented. It is assumed that there can be an upper and lower tolerance in each case, and thus for a problem with N dimensions, it is demonstrated that the solution lies within the common domain of the 2^N+1 possible hyper-surfaces. Furthermore, it is also assumed that the probability of any tolerance value occurring within the tolerance band, compared with any other, is equal, and thus it is a worst-case scenario approach. In order to determine the optimum solution, the technique utilizes a genetic algorithm with fitness sharing, including a micro-genetic algorithm, which has been found to be very suitable (viz. accurate, fast and efficient), particularly when the dimensionality of the problem is high.

In order to demonstrate the technique, the maximization of the burst pressure of a laminated anisotropic cylindrical pressure vessel is considered. The design variables are the ply fibre angles and the layer thicknesses, and thus the examples are considered with tolerances in these variables accounted for. Initially, when one layer is used, the difference between the actual and nominal burst pressure is extreme (60.2%) and this clearly demonstrates the point. When two layers are used, the difference is reduced to 51.68% The point is driven home when one considers specifying the nominal values of the fibre orientations (say in the five ply case) and tolerances are incurred during fabrication: the burst pressure can be as much as 64% less than expected.

References

.

[1] Chao L.P., Gandhi M.V. and Thompson B.S. "A design for manufacture methodology for incorporating manufacturing uncertainties in the robust design of fibrous laminated composite structures". *Journal of Composite Materials,* Vol. 27, No. 2, pp 175-194, 1993.

[2] Bauer J. and Latalski J. "Manufacturing tolerances of truss members' lengths in minimum weight design ". *Computer Assisted Mechanics and Engineering Sciences*, Vol. 7, No. 4, pp 461-469, 2000.

[3] Yunn-Shiuan Liao and Chwei-Yuh Chiou. "Robust optimum design of fiber-reinforced composites using constraints with sensitivity." *Journal of Composite Materials,* Vol. 40, No. 22, pp 2067-2081, 2006. 2006.

[4] Walker M., Hamilton R. "A technique for optimally designing fibre-reinforced laminated plates with manufacturing uncertainties for maximum buckling strength". *Engineering Optimization*, Vol. 37, No. 2, pp 135-144, 2005.

[5] Walker M., Hamilton R. "A methodology for optimally designing fibre-reinforced laminated structures with design variable tolerances for maximum buckling strength". *Thin Walled Structures*, Vol. 43, pp 161-174, 2006.

[6] Tabakov P.Y. and Walker M. "A technique for optimally designing engineering structures with manufacturing tolerances accounted for." *Engineering Optimization,* Vol. 39, No. 1, pp 1-15, 2007.

[7] Tabakov P.Y. and Summers E.B. "Lay-up optimization of multilayered anisotropic cylinders based on a 3-D elasticity solution". Vol. 84, pp 374-384, 2006.

[8] Lekhnitskii S.G. "*Theory of elasticity of an elastic anisotropic body*". San Francisco: Holden-Day, Inc.; 1963. Translated by P.Fern.

[9] Tsai S.W. and Wu E.M. "A general theory of strength of anisotropic materials." *Journal of Composite Materials,* Vol. 5, pp 58-80, 1971.